

PHOTOELASTIC PROPERTIES OF FOUR HEXAGONAL SILICON CARBIDE SINGLE CRYSTAL

Kenji Gomi*, Takahiro Omura, Hiroshi Kusaga, Shota Mori and Kensuke Ichinose*

*Dept. of Mech. Eng., Tokyo Denki University, Kanda Nishiki-cho, 2-2, Chiyoda-ku, Tokyo 101-8457, Japan

Introduction

Four hexagonal silicon carbide (4H-SiC) single crystals have drawn much attention as a material for power devices [1]. For quality control of 4H-SiC wafers, it is important that the estimation of the optical retardation in the wafers corresponds to the residual stress. For this estimation, photoelastic stress-strain measurement is suitable, because photoelasticity has the distinct advantages of being non-destructive, convenient, real-time, precise, and quantitative compared with other stress-strain measurement techniques. To adopt photoelastic stress-strain measurement into the estimation for residual stress in 4H-SiC, the photoelastic properties which depend on the crystalline orientation should be obtained in advance.

Thus, an optical birefringence measurement system is made with a photoelastic modulator and polarized laser. A helium-neon (He-Ne) infrared laser is utilized as the light source for measuring the birefringence in 4H-SiC wafers. In this paper we will explain the principles behind the system and the process for determination of the photoelastic properties in 4H-SiC wafers.

Equipment and Principle of Measurement

Birefringence measurement equipment

Fig. 1 shows the design of the birefringence measuring equipment. This equipment enables the simultaneous measurement of magnitude and direction of the birefringence without the specimen rotation. An 8 mW He-Ne laser beam ($\lambda=1150$ nm)

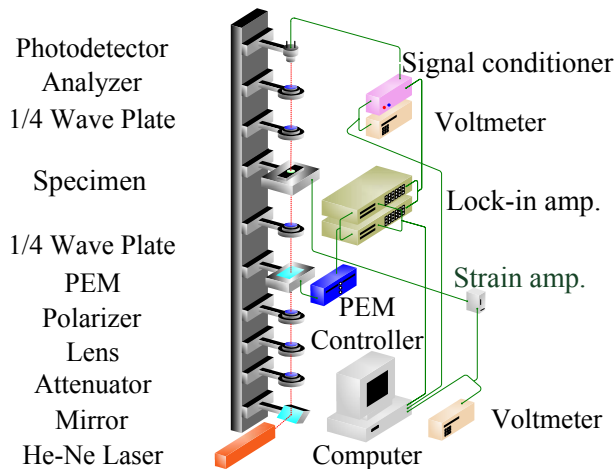


Fig. 1 Birefringence measuring equipment

passes through a polarizer (Glan-Thompson Prism), a PEM (Photo-Elastic Modulator), a quarter wave plate, a 4H-SiC specimen, a quarter wave plate, and an analyzer. After passing through the analyzer, the laser light is measured using a photodetector. The PEM converts linearly polarized light into oscillating elliptic light at its 42 kHz resonant frequency. The direction of the birefringence axis of the PEM inclines 90° from the axis of the analyzer, and 45° from the axis of the polarizer. The directions of the fast axes of the quarter wave plates incline 45° from the axis of the analyzer, and 90° from the axis of the polarizer.

Relation between optical retardation and transmitted light intensity

The light intensity, I , that comes through the analyzer can be expressed as a Fourier's expansion as follows:

$$I = I_{dc} + I_{ac1} \sin \omega t + I_{ac2} \cos 2\omega t + I_{ac3} \sin 3\omega t + \dots \quad (1)$$

$$I_{dc} = (\alpha I_0 / 4) \{1 + J_0(\delta_0) \sin \gamma \sin 2\theta\} \quad (2)$$

$$I_{ac1} = -(\alpha I_0 / 2) J_1(\delta_0) \sin \gamma \cos 2\theta \quad (3)$$

$$I_{ac2} = (\alpha I_0 / 2) J_2(\delta_0) \sin \gamma \sin 2\theta \quad (4)$$

where ω is the 42 kHz resonant frequency of PEM, α is the transparency of the specimen, I_0 is the light intensity before transmission by the polarizer, γ is the retardation of birefringence of the specimen, and θ is the angle of the birefringence axis based on the zero orientation of the lower quarter wave plate in Fig. 1, I_{ac1} and I_{ac2} are the alternating light intensities of the resonance frequency and its double frequency, and I_{dc} is the direct component of the light intensity. Both I_{ac1} and I_{ac2} are measured by lock-in amplifiers. The direct component I_{dc} is measured by a voltmeter. $J_0(\delta_0)$, $J_1(\delta_0)$ and $J_2(\delta_0)$ are Bessel's functions. The second term of Equation (2) can be eliminated by adjusting the PEM voltage, so that the direct component I_{dc} becomes constant and is independent of both the axis angle, θ , and retardation, γ , of the specimen. Dividing Equation (3) and (4) by Equation (2), we can obtain:

$$(I_{ac1} / I_{dc}) = A_1 \sin \gamma \cos 2\theta \quad (5)$$

$$(I_{ac2} / I_{dc}) = A_2 \sin \gamma \sin 2\theta \quad (6)$$

where, A_1 and A_2 are constants which are independent of both the transparency and stress state of the specimen. They are determined by the experimental results using the quarter wave plate as a specimen. They were $A_1 = -0.111$ and $A_2 = 0.0167$.

The values of γ and θ of the specimen are obtained from Equation (5) and (6),

$$\gamma = \sin^{-1} \left\{ \sqrt{\{I_{ac1}/(I_{dc}A_1)\}^2 + \{I_{ac2}/(I_{dc}A_2)\}^2} \right\} \quad (7)$$

$$\theta = 0.5 \tan^{-1} \left\{ (A_1 I_{ac2}) / (A_2 I_{ac1}) \right\} + H(-I_{ac1}) 0.5\pi \quad (8)$$

$$H(x) = 0 \quad (x < 0), 1 \quad (x \geq 0)$$

where γ is the absolute value. The resolution of the retardation measurement is better than 1 nm. The signs of I_{ac1} and I_{ac2} are determined using the phase difference between the applied oscillating PEM voltage and the detected voltage of the photodetector.

Specimens and Experiments

Table 1 shows the properties of the commercial wafers as specimens. To determine the photoelastic coefficients and the relations between the applied stress orientations and induced strain orientations, we prepared strip specimens as shown in Fig. 2 from the wafers. Fig. 3 shows the cutting orientations for the strip specimens for four-point bending as shown in Fig. 2. θ_c s in Fig. 3 correspond to the cutting orientation from [1 1 -2 0] orientation flat. 4H-SiC single crystal is categorized into the hexagonal system, the (0001) surface has rotational symmetry every 60 degrees of θ_c in its physical properties. Therefore, we should examine only in the range of 0-60 degrees of θ_c . Accordingly, we cut the four types of 15-degree steps as shown in Fig. 3. Using these strip specimens, we measured photoelastic properties at the center of the specimens under four-point bending as shown in Fig. 2.

Table 1 Properties of SiC single crystal wafers as specimens

Method of crystal growth	Modified Lely method
Polytype	4H
Orientation of principal plane	(0001)
Conductive type	n-type
Dimensions	$\phi 2' \times 3.7 \times 10^2$ [μm]
Polishing (Si face)	Primary polishing
Polishing (C face)	Primary polishing

Results and Discussion

Fig. 4 shows the relationship between the measured photoelastic constants and applied stress orientation, θ_c . The horizontal and radial axes correspond to the former; the semicircle axis means the latter, respectively. Fig. 5 shows induced strain directions shifted from the applied stress directions. These results should be verified by discussion of the mechanical properties of 4H-SiC.

Conclusion

We measured photoelastic properties to adapt the photoelastic stress strain measurement method to

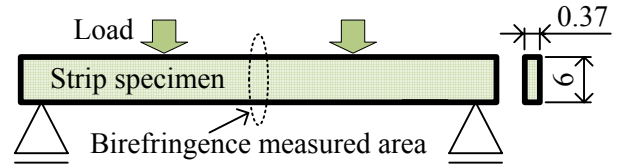


Fig. 2 Strip specimen cut from wafers, its loading points and measured area

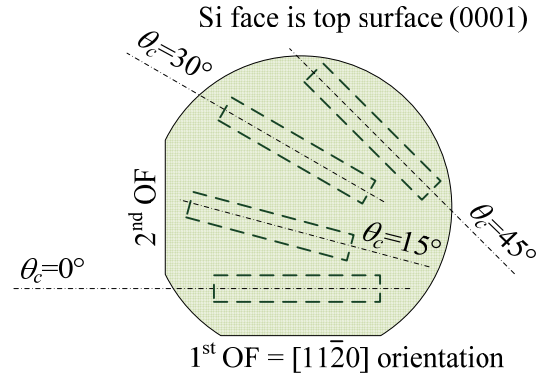


Fig. 3 Strip cutting orientations

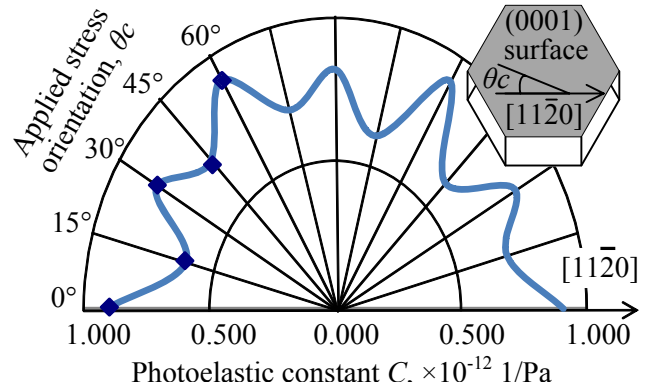


Fig.4 Photoelastic constant of 4H SiC

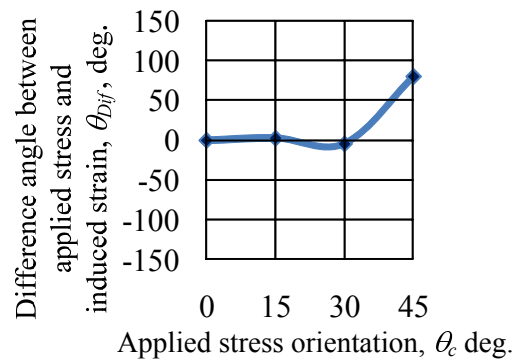


Fig. 5 Angles between stress and strain

quality control of 4H-SiC single crystal wafers. The measured constant was $0.615-0.937 \times 10^{-12} \text{Pa}^{-1}$ as a function of crystalline orientation.

References

1. Kato, T., Photoelastic constant and internal stress and around micropipe defect of 6H-SiC single crystal, *Materials Science and Engineering*, B57 (1999), pp.147-149.